Published by Institute of Physics Publishing for SISSA/ISAS
Received: June 21, 2004
Revised: November 11, 2004
Accepted: December 16, 2004

SNO, SuperKamiokande data, antineutrinos and sterile neutrinos

Bhag C. Chauhan* **and João Pulido**

Centro de Física das Interacções Fundamentais (CFIF), Departamento de Física
Instituto Superior Técnico, Av. Rovisco Pais, P-1049-001 Lisboa, Portugal
E-mail: chauhan@cfif.ist.utl.pt, pulido@cfif.ist.utl.pt

Abstract: Allowing for antineutrinos ($\bar{\nu}_x$) and sterile neutrinos (ν_s) to accompany LMA oscillations, we derive, in a model independent way, upper bounds on their components in the solar flux, using the recent data from SNO and SuperKamiokande. Along with the general case (LMA + $\bar{\nu}_x$ + ν_s) we consider the special cases where only $\bar{\nu}_x$ or ν_s are present. We obtain an upper bound on $\bar{\nu}_x$ which is independent of the ν_s component. In the no sterile case we obtain upper and lower bounds on f_B, the SSM normalization factor. We also investigate in the general case the common parameter range for f_B and the $\bar{\nu}_x$, ν_s components and find that the upper bound on ν_s is hardly sensitive to the $\bar{\nu}_x$ component. In the absence of $\bar{\nu}_x$ we recover the ν_s upper bound existing in the literature. We finally present a simple χ^2 analysis of all four cases considered.

Keywords: Solar and Atmospheric Neutrinos, Neutrino Physics.

*On leave from Govt. Degree College, Karsog (H P) India 171304.

http://jhep.sissa.it/archive/papers/jhep122004040/jhep122004040.pdf

JHEP12(2004)040

Contents

1. Introduction

Despite the recent realization [1] that the solar neutrino deficit, acknowledged over three decades ago [2], results mostly from neutrino oscillations through LMA [3], it is by no means certain whether oscillations are accompanied by the conversion in the sun of electron neutrinos into sterile ones, into antineutrinos of other species, or both. This open question has obvious implications in a possible time modulation of the solar neutrino flux, an effect for which evidence was found by the Stanford Group [4]–[7]. In fact, if electron neutrinos produced in solar fusion reactions interact via a sizeable magnetic moment [8] with a time varying solar magnetic field, the result is the production of a time dependent component of active $\bar{\nu}_\mu$ or $\bar{\nu}_\tau$ or unobserved sterile neutrinos [9] in the neutrino flux from the sun, reflecting in some way the time variation of the solar field.

In this article we perform a model independent analysis of the implications from the SNO salt phase I and II [10] and SuperKamiokande (SK) results [11] on the flux of sterile neutrinos and active antineutrinos which may accompany the LMA effect. Being model independent, our analysis will mainly focus on solar neutrino data and its implications on bounds of sterile neutrino and antineutrino components. Several model independent analyses of solar neutrino data have been performed in the past. These concentrated in the survival probability P_{ee} [12] and sterile neutrino component bounds [13]–[17]. In section 2 we examine the consequences from SNO and SK for the joint possibility of active antineutrinos and sterile neutrinos in the solar flux and for the limiting cases of each of these components alone. So in this respect our results generalize those of ref. [15]. Regarding $\bar{\nu}_e$, all considerations derived for antineutrinos of the other flavours would apply, if not for the recent and very strict upper bound on the former from the KamLAND experiment [18]. We find that SK data on the neutrino electron scattering total rate leads to the exclusion of all active antineutrinos up to 1.17σ and 0.83σ when combined with SNO data from salt phase I and II respectively. Up to 2σ the percentage of non electron antineutrinos $\bar{\nu}_x$ in the active neutrino flux is smaller than 64% and 88% when SK is combined with data from SNO I and II respectively. Our results are independent of standard solar model normalization. Section 3 deals with a simple χ^2 analysis and in section 4 we expound our main conclusions.

JHEP12(2004)040

	CC	NC	ES
SNO I	$0.275\pm^{0.017}_{0.018}$	0.900 ± 0.081	$0.382\pm^{0.056}_{0.048}$
SNO II	$0.294\pm^{0.020}_{0.021}$	$0.846\pm^{0.065}_{0.062}$	$0.368\pm^{0.056}_{0.050}$
SK			$0.406\pm^{0.013}_{0.011}$

Table 1: Ratios of event rates to standard solar model [20] event rates at SNO and SK (theoretical error not considered).

2. Model independent analysis

We start with the event rate expressions for the charged current (CC) and neutral current (NC) reactions for SNO and neutrino electron scattering (ES) for SK, SNO [19]

$$R^{CC} = f_B P_{ee} \tag{2.1}$$
$$R^{NC} = f_B P_{ee} + f_B(1-P_{ee})[\sin^2\alpha \sin^2\psi + \bar{r}_d \sin^2\alpha \ \cos^2\psi] \tag{2.2}$$
$$R^{ES} = f_B P_{ee} + f_B(1-P_{ee})[r \sin^2\alpha \sin^2\psi + \bar{r} \sin^2\alpha \ \cos^2\psi]\,. \tag{2.3}$$

Of all electron neutrinos that are converted, proportional to $1-P_{ee}$, $\sin^2\alpha$ denotes the fraction that is converted into active ones $\nu_x, \bar{\nu}_x$, $(x \neq e)$ while ψ is the angle describing the $\nu_x, \bar{\nu}_x$ components. The sterile neutrino component is therefore proportional to $\cos^2\alpha$. Parameter f_B denotes the normalization to the standard solar model ^8B neutrino flux [20]. Quantities r, $\bar{r}$ are respectively the ratios of the NC neutrino and antineutrino event rates to the NC+CC neutrino event rate and $\bar{r_d}$ is the ratio of the antineutrino deuteron fission to neutrino deuteron fission event rate. Specifically

$$r = \frac{\int dE_\nu \phi(E_\nu) \int dE_e \int dE_e^{'} \frac{d\sigma_{NC}}{dE_e} f(E_e^{'}, E_e)}{\sigma_{NC} \to \sigma_{NC+CC}} \tag{2.4}$$
$$\bar{r} = \frac{\int dE_\nu \phi(E_\nu) \int dE_e \int dE_e^{'} \frac{d\bar{\sigma}_{NC}}{dE_e} f(E_e^{'}, E_e)}{\bar{\sigma}_{NC} \to \sigma_{NC+CC}} \tag{2.5}$$
$$\bar{r}_d = \frac{\int dE_\nu \phi(E_\nu) \bar{\sigma}_{NC}(E_\nu)}{\bar{\sigma}_{NC} \to \sigma_{NC}} \tag{2.6}$$

where f is the energy resolution function for SNO [21] or SK [22]. Owing to its near energy independence in this range, the electron neutrino survival probability P_{ee} is factorized out of these integrals as in eqs. (2.1)–(2.3). Energy thresholds considered are $E_{e_{th}} = 5.5, 5\,\mathrm{MeV}$ for SNO and SK respectively and the rest of the notation is standard. We obtain

$$r = 0.150 \ (0.151 \text{ for SK})\,, \qquad \bar{r} = 0.115 \ (0.116 \text{ for SK})\,, \qquad \bar{r_d} = 0.954\,. \tag{2.7}$$

where these minor differences are mainly the result of the difference in the threshold energies, being largely independent of the resolution functions. The data from SNO (phase I and II) and SK are summarized in table 1.

From eqs. (2.1)–(2.3) one can eliminate the angle α and express angle ψ in terms of the experimental event rates and other model independent quantities,

$$\sin^2\psi = \frac{\bar{r} - \gamma \bar{r_d}}{\gamma(1-\bar{r_d}) + \bar{r} - r} \tag{2.8}$$

JHEP12(2004)040

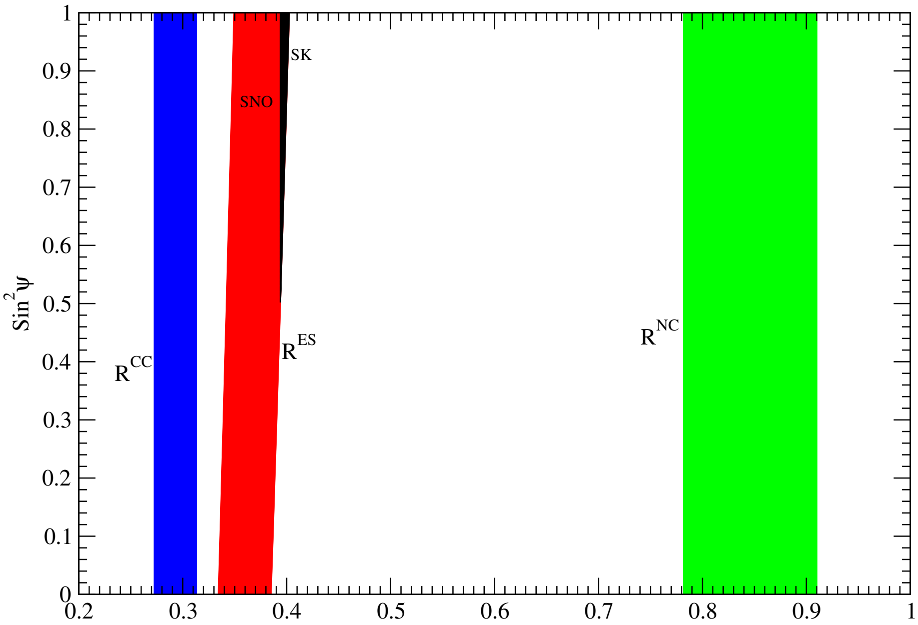

Figure 1: The coloured areas are the regions allowed by the 1σ ranges of the reduced rates, as reported by the SNO II experiment, and $\sin^2\psi$, proportional to the neutrino component of the active non-ν_e flux. The dark shaded area is the region allowed jointly by the SNO II and SK data on the electron scattering reduced rate.

with

$$\gamma = \frac{R^{ES} - R^{CC}}{R^{NC} - R^{CC}}\,. \tag{2.9}$$

If not for the large uncertainties that are propagated into equation (2.8) originated from the uncertainties in R^{ES}, R^{CC}, R^{NC}, this would unambiguously determine the relative proportion of non electron antineutrinos $\bar{\nu}_x$ in the active non ν_e flux. Hence, as will be seen, only upper bounds on the fraction of the $\bar{\nu}_x$ flux can be derived at the present stage. To this end we evaluate the parameter $\sin^2\psi$ using eq. (2.8) for all values of R^{ES}, R^{CC}, R^{NC} within their allowed 1σ ranges for SNO: these are represented by the light shaded areas in figure 1 where the SNO data used are those from salt phase II. Hence for each chosen value of $\sin^2\psi$ the allowed values of the three reduced rates lie within each shaded area. If the SNO experiment alone is considered, it is seen that all possible values of $\sin^2\psi$ in the range $0 \le \sin^2\psi \le 1$ can be obtained. We note that as the $\bar{\nu}_x$ component decreases and eventually vanishes ($\sin^2\psi \to 1$), the factor multiplying r in eq. (2.3) increases while the one multiplying $\bar{r}$ approaches zero. Owing to the relative difference between r and $\bar{r}$ (eq. (2.7)), this implies a slight inclination into larger values of R^{ES} for a decreasing $\bar{\nu}_x$ component. The same effect, although much less significant, because of the much smaller difference between $\bar{r}_d$ and unity, is also present in the $(\sin^2\psi, R^{NC})$ area and does not exist in R^{CC} (see eq. (2.1)).

The data from the SK experiment with R^{ES} restricted to its SK 1σ range (see table 1) are also used to evaluate $\sin^2\psi$. In figure 1 the dark shaded area which is part of the total $(\sin^2\psi, R^{ES})$ one represents the parameter range allowed jointly by SNO II and SK. This

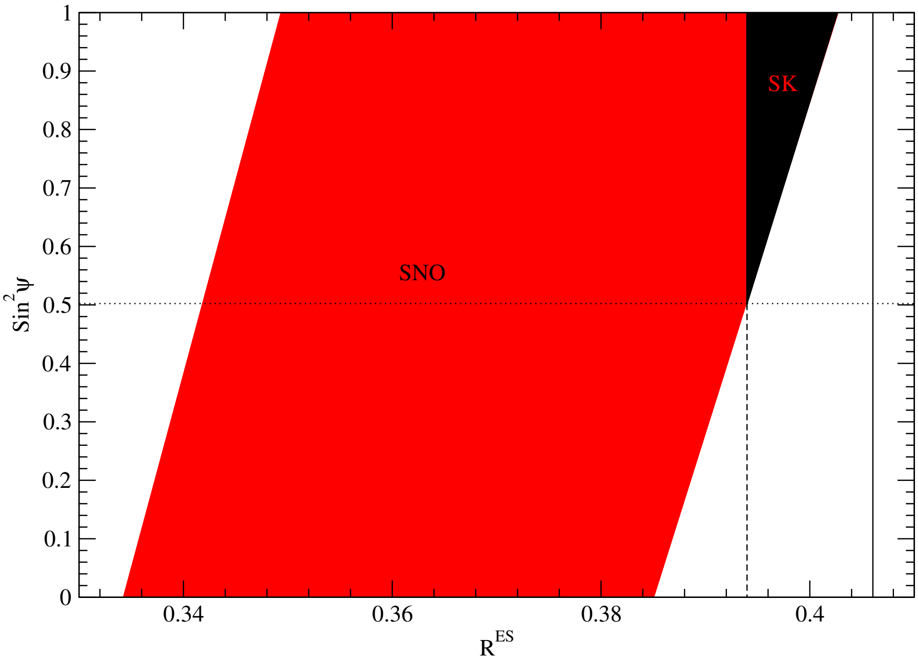

Figure 2: Same as figure 1 with a magnified horizontal scale to show the lower bound on $\sin^2\psi$ implied by the data from the two experiments. This bound is independent from the sterile neutrino component (see also the main text).

is enlarged in figure 2 with a magnified horizontal scale. The result is a lower bound on $\sin^2\psi$

$$\text{SNO II} \quad \sin^2\psi > 0.5 \;\; \text{at } 1.49\sigma (87\% \; CL) \tag{2.10}$$

which is in fact an upper bound (0.5) on the fraction of non-electron antineutrinos $\bar{\nu}_x$ in the active non-ν_e flux.[1] The same procedure, as applied to SNO I with SK leads to

$$\text{SNO I} \quad \sin^2\psi > 0.95 \;\; \text{at } 1.23\sigma (79\% \; CL)\,. \tag{2.11}$$

The upper bound on $\bar{\nu}_x$ is therefore more restrictive (0.05) if one considers SNO I data. Up to 95% CL these bounds become

$$\sin^2\psi > 0.12 \text{ (SNO II)}\,, \quad \sin^2\psi > 0.36 \text{ (SNO I)} \qquad (95\% \; CL) \tag{2.12}$$

hence respectively an upper bound of 0.88 and 0.64 on the $\bar{\nu}_x$ fraction. These results are independent of the normalization to any particular standard solar model. No restriction on the sterile neutrino component, proportional to $\cos^2\alpha$ (see eqs. (2.2), (2.3)), has been considered so far, therefore our analysis is valid for any ν_s, $\bar{\nu}_x$ admixture accompanying the LMA effect. Combining separately eqs. (2.1), (2.2) and eqs. (2.1), (2.3) one can relate the normalization factor f_B to the mixing angles α, ψ. We have respectively

$$f_B = R^{CC} + \frac{R^{NC} - R^{CC}}{\sin^2\alpha(\sin^2\psi + \bar{r}_d\cos^2\psi)} \tag{2.13}$$

[1]Recall that the $\bar{\nu}_x$ component is proportional to $\cos^2\psi$ (see eqs. (2.2), (2.3)).

JHEP12(2004)040

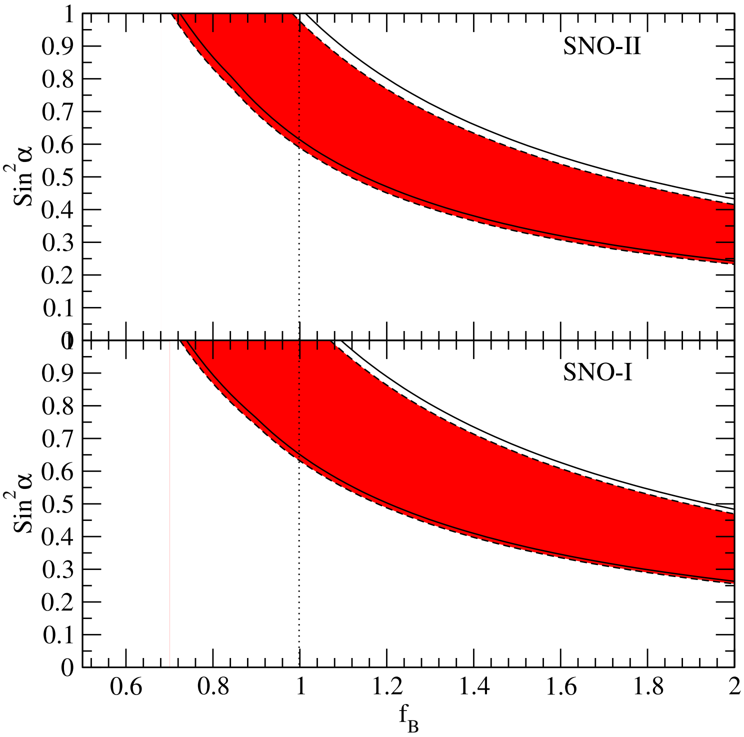

Figure 3: The allowed range at 2σ of $\sin^2\alpha$ (proportional to the total active non-ν_e flux) and f_B, the SSM normalization factor, using SNO II and SNO I data. Dashed lines correspond to absence of antineutrinos, while full lines to their upper bound at 2σ. It is seen that the sterile component, proportional to $\cos^2\alpha$, is hardly affected by the presence of antineutrinos.

$$f_B = R^{CC} + \frac{R^{ES} - R^{CC}}{\sin^2\alpha(r\sin^2\psi + \bar{r}\cos^2\psi)}\,. \tag{2.14}$$

We represent in figure 3 the allowed range of $\sin^2\alpha$ (proportional to the active non-ν_e component) in terms of f_B at the 95% CL for SNO II (figure3a) and SNO I (figure 3*b*) using inequalities (2.12) and eq. (2.13). Considering the two possible equivalent choices to generate figure 3, namely eqs. (2.13) and (2.14), the former should in fact be preferred since it leads to the narrowest error bars in f_B. The dashed and full lines in figure 3 correspond respectively to $\sin^2\psi = 1$ (no antineutrinos $\bar{\nu}_x$) and to the 95% CL upper limits for $\bar{\nu}_x$. These are $\sin^2\psi = 0.12$ for SNO II and $\sin^2\psi = 0.36$ for SNO I (see eq. (2.12)). Hence the existing shift between each adjacent dashed and full line represents the small change in the sterile neutrino component, proportional to $\cos^2\alpha$, resulting from introducing in the scheme a $\bar{\nu}_x$ component up to its 95% CL upper bound. This shows that the possible sterile neutrino flux is hardly sensitive to the presence of antineutrinos, a fact whose origin becomes clear on examination of the denominator in eq. (2.13): the multiplier of $\sin^2\alpha$ is very close to unity for any value of ψ owing to the fact that $\bar{r}_d \simeq 1$. From figure 3 it is also seen that in the absence of $\bar{\nu}_x$ ($x \neq e$, $\sin^2\psi = 1$) the fraction of solar neutrinos oscillating to active ones is greater than 0.59 (SNO II) and 0.63 (SNO I) at 2σ of the non-ν_e flux. Allowing for non-electron antineutrinos up to their 2σ upper bound this fraction becomes respectively 0.62 and 0.66. This result is consistent with the result of ref. [15] where the authors also included KamLAND data in their analysis but were restricted to the case $\sin^2\psi = 1$.

We now take an alternative view by considering separately the cases in which either only $\bar{\nu}_x$ or ν_s is present along with LMA and derive in each the corresponding constraints on the SSM normalization factor f_B. We start with the case where no steriles are present (only $\bar{\nu}_x$). Here $\sin^2\alpha = 1$ and from eqs. (2.2), (2.3) one obtains

$$f_B = R^{CC} + \frac{(R^{NC} - R^{CC})(r - \bar{r}) - (R^{ES} - R^{CC})(1 - \bar{r}_d)}{\bar{r}_d(r - \bar{r}) - \bar{r}(1 - \bar{r}_d)} \tag{2.15}$$

which for SNO II and SNO I give respectively, using table 1 (to 1σ)

$$f_B = 0.86 \pm 0.12 \text{ (SNO II)}\,, \qquad f_B = 0.88 \pm 0.13 \text{ (SNO I)}\,. \tag{2.16}$$

We note that these correspond to the allowed ranges within the lines $\sin^2\alpha = 1$ in figure 3*a* and figure 3*b*, the slight discrepancies with this figure being of course the result of the experimental uncertainties and the different procedures used for generating the two sets of results. For the combined SNO and SK data, eq. (2.16) becomes instead (to 1σ)

$$f_B = 0.80 \pm 0.09 \text{ (SNO II + SK)}\,, \qquad f_B = 0.84 \pm 0.10 \text{ (SNO I + SK)}\,, \tag{2.17}$$

the smaller error resulting from the smaller SK error. All these parameter ranges lie within the allowed 1σ SSM error of 23% [20]. It is thus seen that the former general analysis which includes antineutrinos and steriles, and whose results are summarized in figure 3, leads to more precise predictions for f_B, as only two experimentally measured quantities R^{NC} and R^{CC} are used in contrast to eq. (2.15). In fact, in figure 3, where all quantities are allowed to vary within their 2σ ranges, we have (for $\sin^2\alpha = 1$)

$$f_B = 0.87 \pm 0.15 \text{ (SNO II)}\,, \qquad f_B = 0.91 \pm 0.19 \text{ (SNO I)} \tag{2.18}$$

to be compared with eq. (2.16) where only 1σ ranges are allowed.

We now briefly refer to the other special case, namely the absence of antineutrinos: only steriles are present here along with the LMA effect, hence $\sin^2\psi = 1$. This case corresponds to the shaded areas in figure 3 limited by the two dashed lines and, in contrast to the previous one, no model independent equation can be obtained for f_B, but only a degeneracy relation between f_B and $\sin^2\alpha$. This can be expressed by either of the two equivalent equations

$$f_B = R^{CC} + \frac{R^{NC} - R^{CC}}{\sin^2\alpha} \tag{2.19}$$

$$f_B = R^{CC} + \frac{R^{ES} - R^{CC}}{r\ \sin^2\alpha} \tag{2.20}$$

which correspond to eqs. (2.13) and (2.14) with $\sin^2\psi = 1$. As previously discussed in the general case (LMA + $\bar{\nu}_x$ + ν_s) the main result here is an upper bound on the sterile component. At 2σ this is $\cos^2\alpha < 0.41$ (from SNO II) or 0.38 (from SNO I) of the non-ν_e flux for $f_B = 1$.

JHEP12(2004)040

	f_B	P_{ee}	$\sin^2\alpha$	$\sin^2\psi$	$\chi^2_{\rm min}$
LMA (2 dof)	0.876	0.356	1.0	1.0	1.67
LMA+$\bar\nu_x$ (1 dof)	0.876	0.356	1.0	1.0	1.67
LMA+ν_s (1 dof)	0.961	0.324	0.869	1.0	1.67
LMA+$\bar\nu_x+\nu_s$ (0 dof)	0.989	0.315	0.833	1.0	1.67

Table 2: Results of χ^2 analysis for SNO II.

	f_B	P_{ee}	$\sin^2\alpha$	$\sin^2\psi$	$\chi^2_{\rm min}$
LMA (2 dof)	0.965	0.304	1.0	1.0	2.47
LMA+$\bar\nu_x$ (1 dof)	0.965	0.304	1.0	1.0	2.47
LMA+ν_s (1 dof)	0.965	0.304	1.0	1.0	2.47
LMA+$\bar\nu_x+\nu_s$ (0 dof)	0.969	0.302	0.933	1.0	2.47

Table 3: Results of χ^2 analysis for SNO I.

3. Introducing χ^2 analysis

We refine our results by performing a χ^2 analysis of all four cases considered. The χ^2 definition is quite simple [16]

$$\chi^2=\sum_i \frac{(R_i-R_i^{th})^2}{\delta R_i^2} \tag{3.1}$$

where the sum extends over the four experiments ($i=ES_{SK},ES_{SNO},NC,CC$), R_i, δR_i denote the experimental reduced rates and their errors quoted in table 1, and R_i^{th} are given by eqs. (2.1)–(2.3). The result of the χ^2 minimization is shown in tables 2, 3 for SNO II and SNO I respectively.

Inspection of table 2 (second row) shows that the best fit for case LMA+$\bar\nu_x$ corresponds to the very absence of $\bar\nu_x$ ($\sin^2\psi=1$). It is also seen that allowing for ν_s alone in addition to LMA (third row) as well as LMA+$\bar\nu_x+\nu_s$ (fourth row) leads to a best fit solution with a small although non negligible ν_s component (13% and 17% respectively). Furthermore table 2 also shows that $\chi^2_{\rm min}$ is independent of the values of f_B, P_{ee}, $\sin^2\alpha$. However it depends on $\sin^2\psi$: if in fact we let $\sin^2\psi$ to be unconstrained, an absolute $\chi^2_{\rm min}$ is obtained for an unphysical value of $\sin^2\psi$.[2] As long as $\sin^2\psi$ remains constrained to its physical region ($0\leq\sin^2\psi\leq 1$), $\chi^2_{\rm min}$ is fixed regardless of the values of the other three parameters f_B, P_{ee}, $\sin^2\alpha$. A similar situation is observed in SNO I (see table 3) with the sterile component totally missing ($\sin^2\alpha=1$) in the LMA+ν_s case. This reflects the fact that the parameters f_B, P_{ee}, $\sin^2\alpha$ can be eliminated from eqs. (2.1)–(2.3) so as to express $\sin^2\psi$ ($\bar\nu_x$ component) in terms of experimentally measured quantities only (see eqs. (2.8), (2.9)). Likewise the bounds on $\sin^2\psi$ are independent of the ν_s component and of the other two parameters f_B, P_{ee} (see eqs. (2.10), (2.12)).

Finally, the 2σ upper bound on the sterile component mentioned at the end of section 2 is also shown in the contour plots of figure 4 and corresponds to the lower edge of the light shaded area.

[2] These are $\chi^2_{\rm min}=0.384$, $\sin^2\psi=2.84$ (SNO II) and $\chi^2_{\rm min}=0.133$, $\sin^2\psi=3.17$ (SNO I).

JHEP12(2004)040

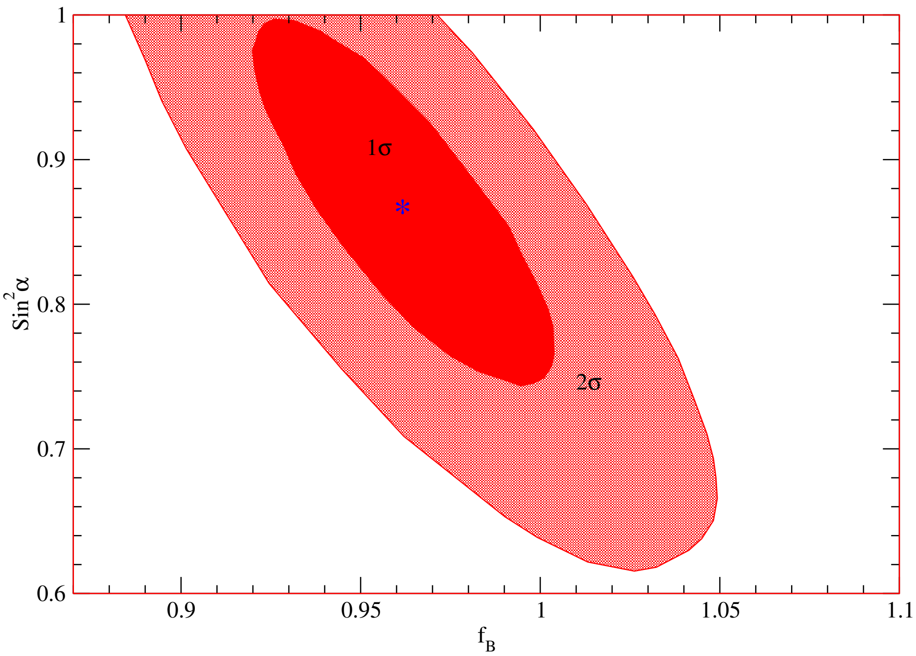

Figure 4: 1σ and 2σ contour plots in the f_B, $\sin^2\alpha$ plane for SNO II data. The star represents the best fit point.

4. Conclusions

To conclude, the results of this paper can be summarized in figures 2, 3 and eqs. (2.16), (2.17), (2.18). Allowing for antineutrinos $\bar{\nu}_x$ other than $\bar{\nu}_e$ and sterile neutrinos, both possibly generated in the sun through spin flavour precession accompanying LMA, we have derived in a model independent way, using SNO and SK data, upper bounds on the flux of these solar antineutrinos and steriles. We related these bounds to the parameter ranges allowed for the SSM normalization factor f_B. To summarize:

- We found an upper bound for $\bar{\nu}_x$ which at 2σ is 0.88 (SNO II) or 0.64 (SNO I) of the active non-ν_e flux (see figure 2 and eq. (2.12)). This is independent of the sterile neutrino component.

- In the no sterile case we obtained upper and lower bounds on f_B (eqs. (2.16), (2.17), (2.18)).

- In the no $\bar{\nu}_x$ case (only steriles accompanying LMA) the fraction of solar neutrinos oscillating to active ones was found to be greater than 0.59 (SNO II) or 0.63 (SNO I) of the non-ν_e flux, a result consistent with ref. [15] which is in fact an upper bound on ν_s.

- Allowing, in the preceding situation, for $\bar{\nu}_x$ up to its 2σ upper bound, these limits are increased by only 5%, (decrease on ν_s upper bound) which shows how the possible ν_s flux is hardly sensitive to the $\bar{\nu}_x$ component.

JHEP12(2004)040

- χ^2 analysis shows that the most disfavoured case (if not excluded) is $\bar{\nu}_x$ either with LMA or with LMA+ν_s. In SNO II it is seen that some possibility is left for LMA+ν_s.

Acknowledgments

The work of B.C.C. was supported by Fundação para a Ciência e a Tecnologia through the grant SFRH /BPD/5719/2001.

References

[1] KamLAND collaboration, K. Eguchi et al., *First results from KamLAND: evidence for reactor anti-neutrino disappearance*, *Phys. Rev. Lett.* **90** (2003) 021802 [hep-ex/0212021].

[2] J. Davis, Raymond, D.S. Harmer and K.C. Hoffman, *Search for neutrinos from the sun*, *Phys. Rev. Lett.* **20** (1968) 1205.

[3] P. Aliani, V. Antonelli, R. Ferrari, M. Picariello and E. Torrente-Lujan, *Analysis of neutrino oscillation data with the recent KamLAND results*, hep-ph/0406182;
A.B. Balantekin and H. Yuksel, *Constraints on neutrino parameters from neutral-current solar neutrino measurements*, *Phys. Rev.* **D 68** (2003) 113002 [hep-ph/0309079];
P. Aliani, V. Antonelli, M. Picariello and E. Torrente-Lujan, *KamLAND potentiality on the determination of neutrino mixing parameters in the post SNO-NC era*, *New J. Phys.* **5** (2003) 2 [hep-ph/0207348];
M. Maltoni, T. Schwetz, M.A. Tortola and J.W.F. Valle, *Status of three-neutrino oscillations after the SNO-salt data*, *Phys. Rev.* **D 68** (2003) 113010 [hep-ph/0309130];
A. Bandyopadhyay, S. Choubey, S. Goswami, S.T. Petcov and D.P. Roy, *Constraints on neutrino oscillation parameters from the SNO salt phase data*, *Phys. Lett.* **B 583** (2004) 134 [hep-ph/0309174];
P. Aliani, V. Antonelli, M. Picariello and E. Torrente-Lujan, *Neutrino mass parameters from KamLAND, SNO and other solar evidence*, *Phys. Rev.* **D 69** (2004) 013005 [hep-ph/0212212];
P.C. de Holanda and A.Y. Smirnov, *Solar neutrinos: the SNO salt phase results and physics of conversion*, *Astropart. Phys.* **21** (2004) 287 [hep-ph/0309299];
J.N. Bahcall, M.C. Gonzalez-Garcia and C. Pena-Garay, *Solar neutrinos before and after KamLAND*, *J. High Energy Phys.* **02** (2003) 009 [hep-ph/0212147].

[4] P.A. Sturrock, D.O. Caldwell, J.D. Scargle, G. Walther and M.S. Wheatland, *Comment on 'search for periodic modulations of the solar neutrino flux in super-Kamiokande i' by Yoo et al*, hep-ph/0403246.

[5] P.A. Sturrock, *Analysis of super-kamiokande 5-day measurements of the solar neutrino flux*, *Astrophys. J.* **605** (2004) 568 [hep-ph/0309239].

[6] D.O. Caldwell and P.A. Sturrock, *New evidence for neutrino flux variability from super-Kamiokande data*, hep-ph/0309191.

[7] P.A. Sturrock and M.A. Weber, *Comparative analysis of GALLEX-GNO solar neutrino data and SOHO/MDI helioseismology data: further evidence for rotational modulation of the solar neutrino flux*, *Astrophys. J.* **565** (2002) 1366 [astro-ph/0103154].

JHEP12(2004)040

[8] C.-S. Lim and W.J. Marciano, *Resonant spin-flavor precession of solar and supernova neutrinos*, *Phys. Rev.* **D 37** (1988) 1368;
E.K. Akhmedov, *Resonance enhancement of the neutrino spin precession in matter and the solar neutrino problem*, *Sov. J. Nucl. Phys.* **48** (1988) 382; *Resonant amplification of neutrino spin rotation in matter and the solar-neutrino problem*, *Phys. Lett.* **B 213** (1988) 64.

[9] B.C. Chauhan and J. Pulido, *LMA and sterile neutrinos: a case for resonance spin flavour precession?*, *J. High Energy Phys.* **06** (2004) 008 [hep-ph/0402194].

[10] SNO collaboration, S.N. Ahmed et al., *Measurement of the total active B-8 solar neutrino flux at the sudbury neutrino observatory with enhanced neutral current sensitivity*, *Phys. Rev. Lett.* **92** (2004) 181301 [nucl-ex/0309004].

[11] Super-Kamiokande collaboration, S. Fukuda et al., *Determination of solar neutrino oscillation parameters using 1496 days of super-Kamiokande-I data*, *Phys. Lett.* **B 539** (2002) 179 [hep-ex/0205075].

[12] V. Berezinsky and M. Lissia, *Electron neutrino survival probability from solar-neutrino data*, *Phys. Lett.* **B 521** (2001) 287 [hep-ph/0108108];
H. Minakata and H. Nunokawa, *Current status of the solar neutrino problem with super-Kamiokande*, *Phys. Rev.* **D 59** (1999) 073004 [hep-ph/9810387].

[13] V.D. Barger, D. Marfatia and K. Whisnant, *Unknowns after the SNO charged-current measurement*, *Phys. Rev. Lett.* **88** (2002) 011302 [hep-ph/0106207].

[14] V. Barger, D. Marfatia, K. Whisnant and B.P. Wood, *Imprint of SNO neutral current data on the solar neutrino problem*, *Phys. Lett.* **B 537** (2002) 179 [hep-ph/0204253].

[15] A.B. Balantekin, V. Barger, D. Marfatia, S. Pakvasa and H. Yuksel, *Physics from future SNO and KamLAND data*, hep-ph/0405019.

[16] V.D. Barger, D. Marfatia and K. Whisnant, *Piecing the solar neutrino puzzle together at SNO*, *Phys. Lett.* **B 509** (2001) 19 [hep-ph/0104166].

[17] M. Cirelli, G. Marandella, A. Strumia and F. Vissani, *Probing oscillations into sterile neutrinos with cosmology, astrophysics and experiments*, hep-ph/0403158.

[18] KamLAND collaboration, K. Eguchi et al., *A high sensitivity search for anti-nu/e's from the sun and other sources at KamLAND*, *Phys. Rev. Lett.* **92** (2004) 071301 [hep-ex/0310047].

[19] S.K. Kang and C.S. Kim, *Implications of SNO and BOREXINO results on neutrino oscillations and majorana magnetic moments*, *Phys. Lett.* **B 584** (2004) 98 [hep-ph/0403059]. These authors take however $\bar{r}_d = 1$ in the equation for R^{NC} [eq. (2.2)].

[20] J.N. Bahcall and M.H. Pinsonneault, *What do we (not) know theoretically about solar neutrino fluxes?*, *Phys. Rev. Lett.* **92** (2004) 121301 [astro-ph/0402114].

[21] SNO website http://sno.phy.queensu.ca/.

[22] SK website http://www-sk.icrr.u-tokyo.ac.jp/doc/sk/ .